ELSEVIER

Diamond and Related Materials 4 (1995) 250–255

DIAMOND AND RELATED MATERIALS

# Step-related growth phenomena on exact and misoriented {001} surfaces of CVD-grown single-crystal diamonds

W. J. P. van Enckevort, G. Janssen, J. J. Schermer, L. J. Giling

*Research Institute of Materials (RIM), University of Nijmegen, Toernooiveld 1, 6525 ED Nijmegen, Netherlands*

**Abstract**

This study gives an overview of growth phenomena observed on {001} homoepitaxial diamond films grown by hot-filament-assisted CVD and acetylene–oxygen flame deposition. The main emphasis lies on the nucleation and propagation of steps, which form a key to understanding the growth on the (2 × 1) reconstructed {001} faces.

*Keywords:* Chemical vapour deposition; Single crystals; Step-controlled epitaxy; Surface characterization

## 1. Introduction

It is now well established that {001} is the appropriate diamond substrate orientation for producing homoepitaxial CVD diamond films with minimal concentrations of point and extended defects [1–3]. To further increase the diamond quality, it is essential to obtain a better understanding of the crystallization mechanism on this surface.

During CVD growth of diamond, the {001} face behaves as an F face owing to its (2 × 1) surface reconstruction by the formation of dimer bonds [4–6]. Therefore growth on the cubic face proceeds via a layer mechanism involving atomic and higher steps. On a perfect crystal, steps can only be generated by the formation of critical, two-dimensional nuclei on the surface. This requires a relatively large supersaturation. However, during the growth of non-perfect crystals, many other sources, such as screw dislocations and foreign particles, may generate steps and growth occurs at much lower supersaturations. Alternatively, it is possible to provide steps by starting with a crystal surface that is slightly misoriented from the exact F-face orientation. This is a common practice in thin-film CVD to obtain high-quality epitaxial layers. After nucleation the steps will advance over the surface. On the {001}(2 × 1) diamond face the steps are preferentially parallel to ⟨110⟩, which is the direction of minimum free energy [4]. These steps can pile up and form bunches or macrosteps.

In this study, the surface morphology of a fairly large number of diamond layers grown on "exact" and on slightly misoriented {001} diamond substrates has been investigated by differential interference contrast microscopy (DICM), scanning electron microscopy (SEM) and atomic force microscopy (AFM). The homoepitaxial diamond films were deposited by conventional hot-filament CVD (HFCVD) [3,7] and the oxygen–acetylene flame method [2,8]. It will be shown that the morphology of the {001} diamond faces and thus their growth is determined by the mechanisms of nucleation and advancement of steps.

## 2. General description of the surface morphologies

The HFCVD-grown layers are relatively thin (5–40 μm), which allows for the study of the initial stages of the growth phenomena. Common features (Fig. 1(a)) on all nearly exact {001} films deposited by HFCVD are (a) more or less square growth hillocks with sides parallel to ⟨110⟩, and (b) randomly oriented, non-epitaxial, three-dimensional diamond nuclei showing {111} and {001} facets [9,10]. On the thinner films these features are separated by flat areas. For thicker films the growth hillocks coalesce (Fig. 1(b)), and finally only the strongest step sources, i.e. the steepest hillocks, will survive. From the narrow size distribution of the hillocks and the three-dimensional nuclei, it can be deduced that their development started at the initial stages of crystal growth. The flat areas between the large growth hillocks are covered by small and shallow growth hillocks in the case of exact {001} surfaces, and by a pattern of shallow lines related to very low steps for


*SSDI* 0925-9635(94)05201-8

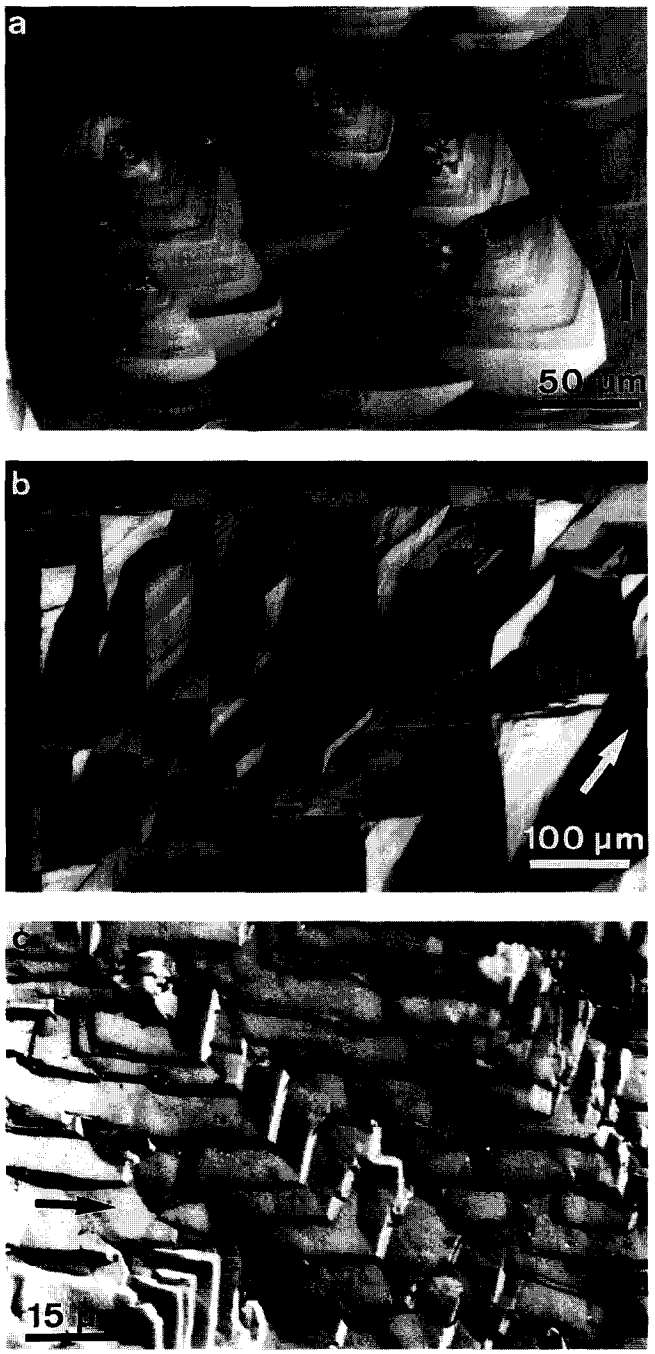


Fig. 1. Typical surface morphologies of diamond films on near-exact {001} as observed by DICM: (a) HFCVD-grown film, about 2° misoriented towards ⟨110⟩ ($T_{fil}$ = 2470 °C, $T_{dep} \approx 850$ °C, $CH_4$:$H_2$ = 2%); (b) HFCVD-grown film with row of hillocks near the edge ($T_{fil}$ = 2460 °C, $T_{dep} \approx 650$ °C, $CH_4$:$H_2$ = 1%); (c) flame-grown film 370 µm thick ($T_{dep}$ = 1200 °C, $S_{ac}$ = 5.4%). Arrows indicate ⟨110⟩ directions.

slightly misoriented faces [10]. Parallel to the rims of the crystal, often a row of growth hillocks (Fig. 1(b)) and/or three-dimensional defects can be seen.

The growth phenomena at a mature stage of development were studied on the thicker layers (100–400 µm) produced by the acetylene–oxygen flame method. The diamond layers on nearly exact {001} substrates usually show macro-steps with the steps aligned along the ⟨110⟩ directions (Fig. 1(c)) [2]. These macro-steps are typically a few micrometers wide and have an inclination between 5° and 20° with respect to the substrate. In contrast to the HFCVD-grown samples, only occasionally are a few, large growth hillocks observed, mostly near the edges of the crystals. On the edges between two adjacent {001} faces, "cusps" can be observed (Figs. 2(a), 2(b)). These are re-entrant corners bounded by two {111} faces and are usually accompanied by penetration twins. Similar, but much smaller, features have been observed at the rims of some of the thickest HFCVD-grown films (Fig. 3(b)). On flame-grown layers, the activity of the step sources is not uniform over the whole {001} surface area. Compared with the central region, generally more steps are generated near the periphery of the surface, which finally leads to concave {001} layers.

## 3. Step nucleation

The growth rate of an F face is proportional to the density of steps times their propagation velocity. Knowledge of the sources of steps provides information on the density of steps. From the surface morphology of the specimens it follows that the sources of steps can be classified in three main groups: hillocks, crystal edges and misorientation of the substrate.

It is obvious that a growth hillock develops around some kind of defect which is capable of continuously creating steps at a higher rate than its surroundings. Inspection of the summits of the hillocks by DICM and AFM shows that at least three types of defects are important, namely foreign diamond crystallites, penetration twins and dislocations.

Sometimes the centre contains a single foreign diamond crystallite, and steps are generated by contact nucleation. In this the activation barrier for two-dimensional nucleation is lowered by the presence of a re-entrant corner at the intersection line of the particle and the {001} surface. In most cases the top is rough in an ill-defined way. AFM shows that this roughness is caused by the close grouping of penetration twins [11,12] and randomly oriented diamond particles (Fig. 3(a)). On such an extended hillock centre, steps are often generated at several discrete points, join and finally form a single growth hillock. Part of these steps is generated by contact nucleation on the low inclination side (= twin plane) of the penetration twins, as indicated by the arrows in Fig. 3(a). A similar step nucleation from twin boundaries is well known for silicon growing from the melt according to the twin-plane re-entrant edge nucleation [13]. It is interesting to note that most of the three-dimensional diamond nuclei and some of

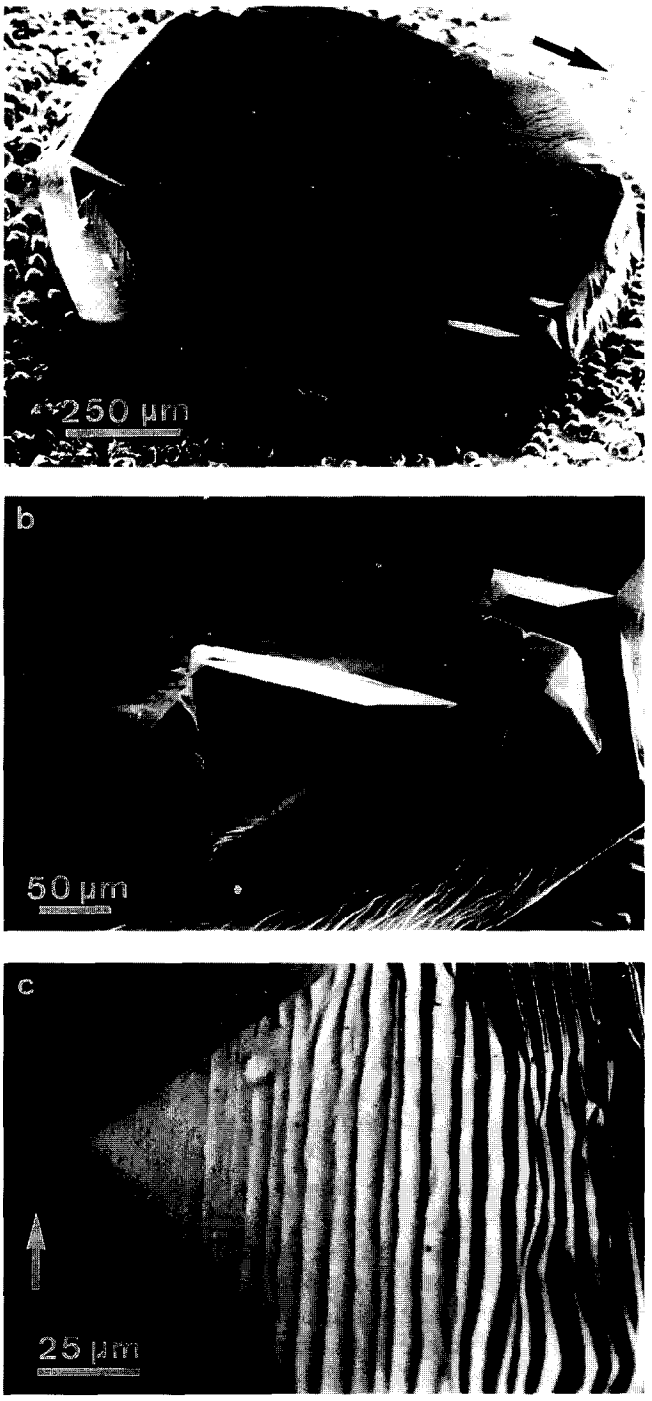


Fig. 2. Step sources on a {001} flame-deposited diamond film ($T_{dep}$ = 1200 °C, $S_{ac}$ = 4%): (a) SEM image of surface morphology of a layer grown on a substrate with a misorientation of 4° towards {100}; (b) SEM image of detail of (a) showing a cusp on the edge with one of the {100} side faces; (c) DICM image of detail of (a) showing a large growth hillock on the top face. Arrows indicate ⟨110⟩ directions.

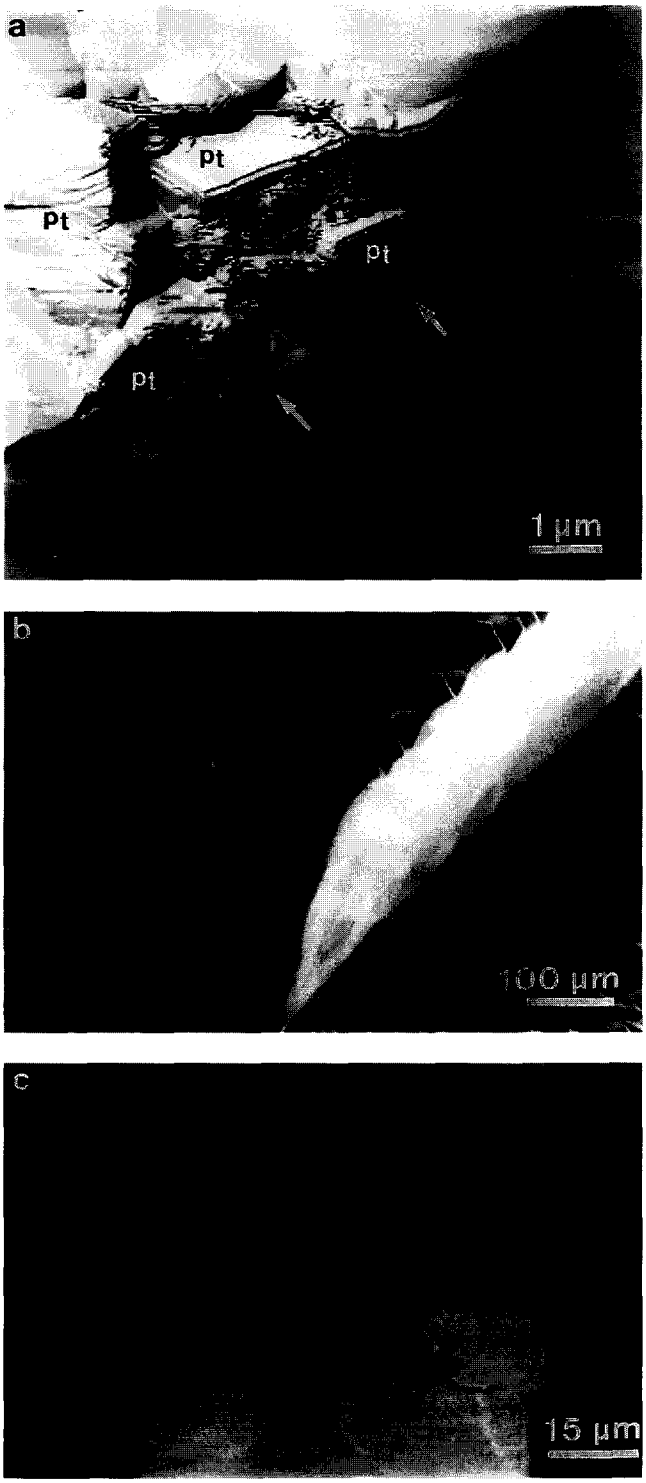


Fig. 3. Step sources on {001} diamond films grown by HFCVD: (a) AFM image of rough top of a growth hillock with penetration twins (pt) and contact nucleation (arrows) ($T_{fil}$ = 2325 °C, $T_{dep}$ = 825 °C, $CH_4$:$H_2$ = 3%); (b) SEM view along the [111] direction showing cusps between three adjacent {001} faces on a layer 40 µm thick ($T_{fil}$ = 2460 °C, $T_{dep} \approx 650$ °C, $CH_4$:$H_2$ = 1%); (c) DICM image of rounded spirals consisting of macrosteps about 70 nm high on a layer about 200 µm thick ($T_{fil}$ = 2700 °C, $T_{dep} > 1000$ °C, $CH_4$:$H_2$ = 2%).

the larger penetration twins that can be identified by DICM are not associated with hillocks. This means that the activity of these particles to generate steps is less than that of adjacent step sources, possibly because of a different orientation of these defects relative to the substrate.

Some of the growth hillocks have a top free from foreign particles and twins (Figs. 1(b), 2(c)). On such hillocks, macrosteps can be observed which emerge from the centre in a spiral pattern (Fig. 3(c)). The step height (60–100 nm) implies that the spirals are due to a large number of closely spaced, cooperating dislocations with a net screw component of the Burgers vector perpendicular to the surface of 60–100 nm. On the other hand, the small and shallow hillocks on exact {001} are thought to be induced by one or a few dislocations outcropping at the substrate surface [10], but isolated steps have not yet been revealed.

The second major group of step sources is situated near the edges of the substrates. During cutting and polishing of the substrate imperfections, strain and sub-micron fracture are introduced at the edges. Furthermore, owing to electrostatic charging or surface-energy lowering, contamination easily accumulates on the very sharp edges. Upon overgrowth of these defective regions, three-dimensional nuclei, twins and dislocations are easily introduced. This gives the same type of step sources as in the first group. Fig. 1(b) presents a row of hillocks introduced in this way, which are parallel but well separated from the edges. Close examination shows that the summits of these elevations are located above the original edges of the substrate. This indicates that the step sources are linear defects which propagate perpendicular to the {001} surface during growth. It is well known for many crystals that, owing to minimization of their line energy, dislocations tend to end perpendicular to a growth face [14]. Therefore the hillocks near the crystal edges are probably growth spirals. In contrast to the hillocks, the "cusps" at the intersection line of two adjacent {001} faces (Figs. 2(a), 2(b), 3(b)) move along with the crystal edge. The cusps which form elevations with the shape of half a growth hillock on both the adjacent {001} facets act as step sources (Fig. 3(b)).

Although a misorientation of the substrate from the exact {001} plane is not an active step source itself, the large number of existing steps will compete with the active step sources. For small misorientations (2° to 3°), many hillocks on HFCVD-grown layers survive, but become deformed (Fig. 1(a)). For misorientations exceeding the maximal hillock slopes of about 4°, the typical defects of the exact layers are completely overrun by the high-density step train of the misoriented surfaces, and become more or less smooth. For flame-grown samples, steps resulting from a misorientation compete with the step sources near the edges and a less concave or even straight layer develops (Fig. 2(a)).

Concerning the activity of the step sources which generate the growth hillocks on HFCVD-grown diamond films, two interesting phenomena were observed. First, for the greater part of all hillocks on a given specimen, the slopes are very similar. Typical inclinations are between 1.5° and 4° relative to the exact {001} plane, with a spread of about 0.5° over a specimen. In view of the large diversity of possible step sources, this is unexpected. A possible explanation might be given by a stabilization of vicinal faces of certain misorientations by surface reconstruction [15,16]. Second, the activity of step sources is not always constant in time. The DICM images of many growth hillocks show patterns of concentric bands (Fig. 1(a)) which are indicative of abrupt and distinct changes in the slope of the hillocks.

AFM [17] shows that the slope of a given hillock face is fairly constant, except for narrow regions (typically 1 μm) with small inclinations approaching zero. These regions cause the band pattern around the four hillock slopes visible by DICM, and indicate that the rate of step generation in the centre changed abruptly and was temporarily very low. Sometimes the activity of the step source does not return to its original value, and a growth hillock with a flattened top develops. In the case of a misoriented substrate, the hillock is then overrun by the steps introduced by the misorientation. This produces the oval-shaped structures in Fig. 1(a) [10]. The reason for the "on–off switching" of the step nucleation activity is as yet unclear. It can however be ruled out that a macroscopic external factor, e.g. fluctuations in the supersaturation, is responsible, as the band pattern of each hillock on a specimen was found to be unique, while flat-topped or oval hillocks occur simultaneously in all stages of development.

## 4. Step anisotropy and step propagation

After propagating some distance, the steps on {001} have a tendency to become aligned parallel to the ⟨110⟩ directions in accordance with the PBC theory and the (2 × 1) reconstruction [4]. Steps in other directions — especially those close to ⟨100⟩, which have a maximal density of kink sites — are undulated [9,10] and will finally break up into perpendicular ⟨110⟩ steps (Fig. 1(c)) [2,16].

Following the notation of Chadi [18] the ⟨110⟩ steps on the {001} faces can be monoatomic ($S$, $h_s = 0.89$ Å) or diatomic ($D$, $h_d = 1.78$ Å) in height, and the direction of the dimer bonds (on the upper terrace) is either perpendicular (A) or parallel (B) to the step. All these step configurations have indeed been observed by scanning tunneling microscopy on CVD-grown diamond [5,19]. Similar to the case of {001} silicon [20], it is

expected that diamond growth is dominated by one type of double step, as the faster of the two possible single steps will catch up the slower one, forming a double step [1].

First attention was focused on surface structures for which the density of steps shows local changes [10]. If surface diffusion is rate-limiting in growth, then, owing to overlapping diffusion fields around adjacent steps, closely separated steps advance slower than those with wider separation. According to the kinematic wave theory of step motion [21], this implies that discontinuous transitions from regions of high step densities to regions of low step densities fade out, whereas the — opposite — discontinuities from low to high step densities remain. If the step velocity is independent of step distance, both kind of discontinuous transitions will persist. From the occurrence of discontinuities in slope on both sides of the oval remains of flat-topped hillocks (Fig. 1(a)), and long persistence of the sharp discontinuities in the band patterns of the growth hillocks, it follows that neighboring steps do not interact [10]. This means that the step velocity is limited either by integration of growth units at the steps or by surface diffusion in which the diffusion fields do not overlap. In the second case, the upper limit for the mean surface diffusion distance is about 1 nm, which implies that the supersaturation in the areas between the steps is relatively high. This may lead to two-dimensional nucleation between the steps as proposed by Tsuno et al. [19].

Next the two-dimensional outer shape of the growth hillocks and spirals on the {001} diamond faces was compared with the theoretical shape of steps far away from the nucleation centre [22]. The calculated morphology was obtained by application of the so-called Gibbs–Wulff operator on a given relation between step velocity and step orientation. The orientation-dependent step velocity follows from a series coupling of surface diffusion of growth units towards the steps and integration of these species in the steps. Following Burton et al. [23], the resistance of the step integration is assumed to be inversely proportional to the density of kink sites, which in turn is a function of step orientation and $\eta = \phi/kT$. Here $\phi$ is the formation energy of a kink position on a step, $k$ is Boltzmann's constant and $T$ is the temperature.

Fig. 4 summarizes some results for different $\eta$ in the absence of surface diffusion. If the relative importance of surface diffusion as a rate-limiting factor increases, then the profiles become, especially near the corners, more rounded. Experimentally the shape of the hillocks on HFCVD-grown layers is influenced by the deposition temperature and the methane fraction in the gas phase. For increasing substrate temperatures the elevations change from exactly square at 650 °C (Fig. 1(b)) via square with rounded corners at 850 °C (Fig. 1(a)) to circular at $T > 1000$ °C (Fig. 3(c)). Some preliminary

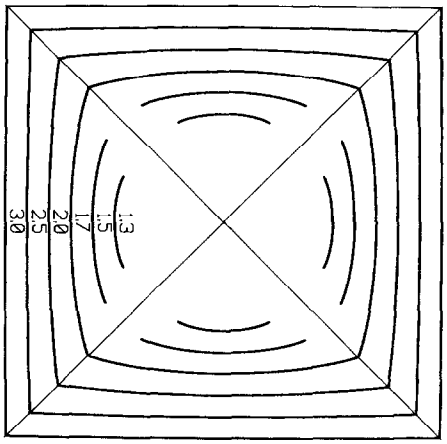


Fig. 4. Theoretical shapes of step patterns far away from their nucleation centre, calculated for various values of $\eta$ in the absence of surface diffusion [22].

fitting of experimental data to the theory indicates that, for the lower temperatures, step integration is at least three times more important as rate-determining step than surface diffusion. The dimensionless kink energy was determined to be $\eta > 2.5$ at 650 °C and $\eta \approx 1.8$ at 850 °C. The circular spirals at $T > 1000$ °C suggest $\eta < 1.4$, but here isotropic surface diffusion can also play a role. The corresponding kink energies of 0.2 eV, 0.17 eV and 0.15 eV are very low compared with the strength of the C–C bond for diamond and adsorbates (about 4.0 eV) or the dimer bond (1.2 eV [24]). This indicates that a kink position does not correspond to a broken dimer bond, but rather to a missing adjacent dimer in the step.

In contrast to the HFCVD-grown material, the growth hillocks on flame-grown diamond films are always square, although the normal deposition temperatures in the flame are significantly higher than during HFCVD (1200 °C compared to 800 °C). The only reasonable explanation is that the kink energy of a step on {001} is different for the two methods, possibly because the geometry of the step has changed or because different adsorbates, e.g. oxygen, are present. The theory shows that, during flame growth, $\eta$ should be larger than about 3, or $\phi \geqslant 0.4$ eV.

In contrast to the HFCVD-grown diamond films, the flame-grown films reveal the occurrence of bunching and macrosteps. Bunching means that successive steps propagating across the surface catch up with a step which has slowed down, e.g. by impurities adsorbed on the surface. Fig. 2(c) clearly shows an example of a growth centre emitting low steps which finally collide to macrosteps. However, for most macrosteps on flame-grown material (Fig. 1(c)) it is less obvious that these are formed by bunching. Already very close to the step source a fully developed macrostep is present, which does not change significantly in height on advancing

across the surface. Similar patterns were observed by Everson and Tamor [25] at hillocks generated by what they call "gross defects" on {001} layers grown by microwave-plasma-assisted CVD. It seems that the phenomenon is related to a fast generation of steps and a large driving force for the formation and stabilization of macrosteps with a specific geometry.

Recently it was observed that, during flame growth above 1150 °C, macroscopic facets in the ⟨110⟩ zones between {113} [26] and {001} are stabilized in two directions [27]. The occurrence of this phenomenon was explained by the possibility for a discrete number of orientations to lower their surface free energy with respect to all their neighboring orientations by dimer formation perpendicular to the ⟨110⟩ PBCs, i.e. $D_A$ steps [16]. As was also proposed by others [15], a similar stabilization might occur for the inclined faces at the macrosteps, since the distinct and abrupt changes in slope of the diamond layers are not expected if the surface is reconstructed by dimers parallel to the ⟨110⟩ PBCs, i.e. $D_B$ steps. Because of large step fluxes due to a fast generation of steps, the situation at the crystal surface goes further from equilibrium, where only $D_B$ steps are expected [18], and the occurrence of $D_A$ steps is favored. These steps pile up and form one of the faces in the ⟨110⟩ zone between {001} and {113} which are stabilized in two directions [16].

## 5. Conclusions

Homoepitaxial growth on the {001} diamond face by CVD processes is controlled by the nucleation and propagation of, mostly, ⟨110⟩-oriented steps. At least three different active steps sources have been identified, namely nucleation on dislocations leading to spiral growth, contact nucleation on non-epitaxial diamond particles and contact nucleation on penetration twins. These steps sources generate large hillocks on HFCVD-grown diamond layers and macro-steps on flame-grown material. The edges of the crystals show "cusps" and enhanced densities of step sources, which is probably due to the presence of defects resulting from strain and work damage.

Finally it must be concluded that a good understanding of the diamond CVD process is impeded by the lack of knowledge on two key parameters in crystal growth, namely the supersaturation and the step free energy. A major effort to solve this theoretical problem seems essential for increasing diamond quality in the future.

## Acknowledgements

The authors thank Mr. W. Elst for technical assistance and Mr. M. da Silva Couto for making the AFM topographs. The BRITE EURAM II program is acknowledged for partial financial support under contract BE2-CT92-0147.

## References

[1] W.J.P. van Enckevort, G. Janssen, W. Vollenberg, J.J. Schermer, L.J. Giling and M. Seal, *Diamond Relat. Mater., 2* (1993) 997.
[2] J.J. Schermer, W.J.P. van Enckevort and L.J. Giling, *Diamond Relat. Mater., 3* (1994) 408.
[3] G. Janssen, W.J.P. van Enckevort, W. Vollenberg and L.J. Giling, *J. Cryst. Growth* (1994), in press.
[4] L.J. Giling and W.J.P. van Enckevort, *Surf. Sci., 161* (1985) 567.
[5] T. Tsuno, T. Imai, Y. Nishibayashi, K. Hamada and N. Fujimori, *Jpn. J. Appl. Phys., 30* (1991) 1063.
[6] L.F. Sutcu, M.S. Thompson, C.J. Chu, R.H. Hauge, J.L. Margrave and M.P. D'Evelyn, *Appl. Phys. Lett., 60* (1992) 1685.
[7] G. Janssen, Homoepitaxial diamond: synthesized by CVD processes, *Thesis*, University of Nijmegen, 1994.
[8] J.J. Schermer, J.E.M. Hogenkamp, G.C.J. Otter, G. Janssen, W.J.P. van Enckevort and L.J. Giling, *Diamond Relat. Mater., 2* (1993) 1149.
[9] W.J.P. van Enckevort, G. Janssen, W. Vollenberg, M. Chermin, L.J. Giling and M. Seal, *Surf. Coat. Technol., 47* (1991) 39.
[10] W.J.P. van Enckevort, G. Janssen, W. Vollenberg and L.J. Giling, *J. Cryst. Growth* (1994), in press.
[11] R.E. Clausing, L. Heatherly, L.L. Horton, E.D. Specht, G.M. Begun and Z.L. Wang, *Diamond Relat. Mater., 1* (1992) 411.
[12] C. Wild, R. Kohl, N. Herres, W. Müller-Sebert and P. Koidl, *Diamond Relat. Mater., 3* (1994) 373.
[13] D.R. Hamilton and R.G. Seidenstich, *J. Appl. Phys., 31* (1960) 1165.
[14] H. Klapper, in B.K. Tanner and D.K. Bowden (eds.), *Characterisation of Crystal Growth Defects by X-ray Methods*, Plenum, New York, 1980, pp. 133–158.
[15] M.A. Tamor and M.P. Everson, *J. Mater. Res., 8* (1993) 1770.
[16] J.J. Schermer, W.J.P. van Enckevort and L.J. Giling, *J. Cryst. Growth*, in press.
[17] G. Janssen, M. da Silva Couto, W.J.P van Enckevort and L.J. Giling, unpublished work, 1994.
[18] D.J. Chadi, *Phys. Rev. Lett., 59* (1987) 1691.
[19] T. Tsuno, T. Tomikawa, S. Shikata, T. Imai and N. Fujimori, *Appl. Phys. Lett., 64* (1994) 572.
[20] A.J. Hoeven, J.M. Lenssinck, D. Dijkkamp, E.J. van Loenen and J. Dieleman, *Phys. Rev. Lett., 63* (1989) 1830.
[21] P. van der Putte, W.J.P van Enckevort, L.J. Giling and J. Bloem, *J. Cryst. Growth, 43* (1978) 659.
[22] W.J.P. van Enckevort, unpublished work, 1994.
[23] W.K. Burton, N. Cabrera and F.C. Frank, *Philos. Trans. R. Soc. London, 243* (1951) 299.
[24] Z. Jing and J.L. Whitten, *Surf. Sci., 314* (1994) 300.
[25] M.P. Everson and M.A. Tamor, *J. Mater. Res., 7* (1992) 1438.
[26] G. Janssen, J.J. Schermer, W.J.P van Enckevort and L.J. Giling, *J. Cryst. Growth, 125* (1992) 42.
[27] J.J. Schermer, P. Alers and L.J. Giling, submitted for publication in *J. Appl. Phys.*